BEAM MEASUREMENTS WITH CRYOINSERTS IN SIS18

L.H.J. Bozyk*[1], P.J. Spiller[1]
[1]GSI Helmholtzzentrum für Schwerionenforschung, Darmstadt, Germany

Abstract

In oder to increase the maximum achievable intensity of medium charge state heavy ion beams in SIS18 at GSI for FAIR-operation, the installation of cryoinserts is foreseen. These cryogenic surfaces with high sticking probability provide high pumping speed around the ion-catcher, where most of the beam-loss induced gas desorption takes place. Such, gas particles get quickly removed, minimizing beam loss by charge exchange from interaction with the residual gas.

A prototype cryoinsert was designed, manufactured and tested, showing the clear reduction of artificial gas pulses. Most recently, the prototype was installed into SIS18. There, a reduction of the static pressure extending several meters after cooldown was observed.

In 2025 the first beam experiments with medium charged Uranium beams and the cryoinserts took place to observe their influence. The charge exchange could be measured, showing a significant decrease due to the cryoinserts and also a slight influence on the transmission in an acceleration cycle was measurable. In the meantime, a series production of cryoinserts is prepared, including improvements and simplifications of the design.

MOTIVATION AND INTRODUCTION

Serving as a booster synchrotron for FAIR, SIS18 will have to provide $1.5 \cdot 10^{11}$ particles per pulse to reach $5 \cdot 10^{11}$ particles in SIS100. To reach these intensities, medium charge state heavy ions like U^{28+} have to be used which avoid stripping losses in the transfer channel and shift the space charge limit to higher number of particles. Unfortunately the probability of charge exchange in collisions with residual gas particles for such ions is much higher, than for higher charge states like U^{73+}. As charge exchanged ions have a different magnetic rigidity than the reference ion, they get separated from the circulating beam. When they are lost at a grazing incidence on the vacuum chamber wall, they release a huge amount of gas via ion impact induced gas desorption. This local increase of residual gas density in turn increases the probability for further charge exchange and gives rise to a self-amplification up to complete beam loss. In this case, the residual gas density is no longer constant during operation, but a *dynamic vacuum* develops. It limits the maximum achievable intensity of heavy ion beams.

There are several technical measures to shift this limit, like lowering the static gas density or the installation of low desorbing surfaces, which is applied in the ion catchers, see [1]. The intensity of SIS18 could be increased significantly [1,2], but the FAIR-intensities are not yet reached. However, simulations using cryogenic surfaces hint, that they would help to increase the maximum intensity [3]. The sticking probability on cryogenic surfaces is close to one and such much higher than on NEG surfaces.

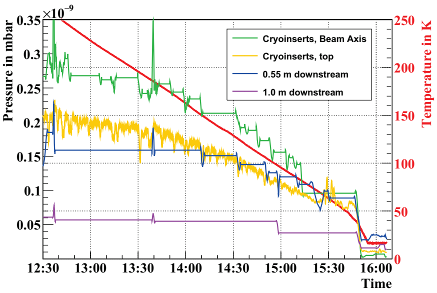

Figure 1: Temperature (red) and pressure evolution at the cryoinserts and at neighboring positions downstream.

A prototype with cryogenic inserts has been set up and tested. It is described in [4,5]. It contains gold-coated copper surfaces, which are cooled by a commercially available cold head. This cold head can be removed without breaking the beam vacuum for the vacuum-bakeout. It has been installed in SIS18 and could be successfully tested without beam, showing significant decrease of the residual gas density [6].

MEASUREMENTS IN SIS18

In July 2025 the cryoinserts could be tested for the first time with medium charged Uranium beams, U^{28+}. The tests were performed within three different cooldowns, each lasting for almost 8 hours. During two of these cooldowns, the lifetime was measured continuously by repetitive storing of low intensity beams for 10 s at injection energy. Alternating to these cycles, high intensity beams with $2-3 \cdot 10^{10}$ injected particles were stored to measure collimator currents. Before and after cooldown respectively, the intensity dependent transmission for different ramping rates was measured.

Figure 1 shows pressure evolution during a cooldown in Section 01, where the cryoinserts are located. The cryoinsert's temperature is shown as well. The continuous decrease of pressure is followed by a sudden drop, when the Hydrogen pumping emerges below 40 K [5].

MEASUREMENT RESULTS

Lifetime Measurements

An increase of lifetime indicating vacuum relaxation after high loss operation during beam setup could be observed. Apart from this effect, no clear signs of lifetime improvement can be seen. The alternating high intensity cycles spoiled the beam life time. Nevertheless, moving the gate valve next to the cryoinserts induces a pressure bump, whose decrease can be investigated by lifetime measurements. Figure 2 shows lifetime evolution at three different temperatures. The lower

---

* L.Bozyk@gsi.de

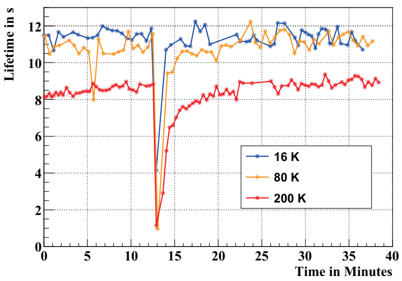

Figure 2: Lifetime evolution at three different temperatures before and after valve movement next to the cryoinserts.

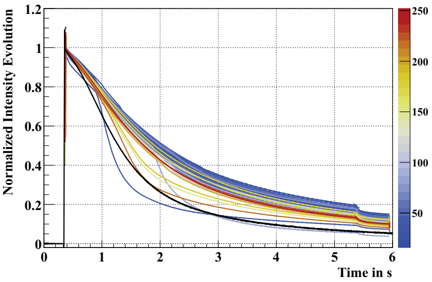

Figure 3: Evolution of normalized intensity during high intensity ($2-3\cdot10^{10}$ particles) storage cycles. The colour code represents the cryoinsert's temperature in K. The cooldown results in slightly improved storage efficiency.

the temperature, the higher the lifetime and the shorter the time to return to the lifetime before valve movement.

Beam Intensity - Storage Mode

The evolution of the normalized intensity in high intensity storage cycles is shown in Fig. 3. Cooling down the cryoinserts results in slightly improved storage efficiency. The black line represents a typical cycle of a previous measurement with comparable intensity before the installation of the cryoinserts. Nevertheless, the stored intensity is above the capabilities of the vacuum system, resulting in the fast intensity drop within the first second.

Collimator Currents

The most explicit result is the measurement of collimator currents [7]. The high intensity storage cycles yield in a clearly measurable charge exchange signal on the electrically insulated collimator block. The collimator currents in the Section 02, subsequent to the cryoinserts were analyzed for Fig. 4. Normalized to the actual beam intensity, they show the dynamic of residual gas density in the vicinity of the cryoinserts. A clear signal decrease with decreasing temperature is visible.

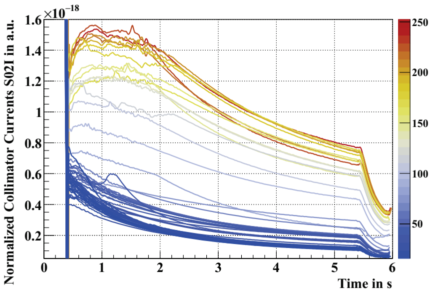

Figure 4: Intensity normalized currents on the (electron loss) collimator collimator subsequent the cryoinserts. The colour code represents the cryoinserts's temperature in K.

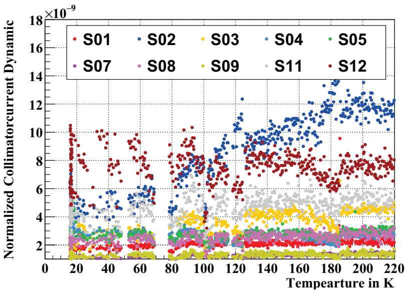

Figure 5: Evolution of collimator current dynamic as a function of the cryoinserts' temperature.

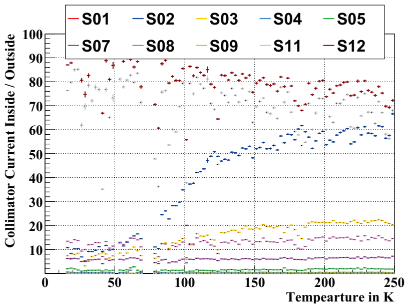

Figure 6: Evolution of current ratio between inside and outside as a function of the cryoinserts' temperature.

Figure 5 shows the dynamic, i.e. difference between max. and min. value, within a cycle as a function of the cryoinsert's temperature. While in all other sections the dynamics remain constant, in S02 the dynamics constantly decrease with decreasing temperature in S01. It is remarkable, that no step occurs with falling temperature, as in the residual gas density shown in Fig. 1. This step is caused by the emerging of Hydrogen-pumping. But as the charge exchange cross sections for Hydrogen are by more than a factor 10 lower, than for all other gas species [8], this additional pumping has only minor influence on the charge exchange rate.

The ratio between the signal inside and outside is influenced by the residual gas composition. Figure 6 shows averaged ratios between electron loss and electron capture of all sections as a function of the cryoinsert's temperature. Obviously two different types of gas composition exist in SIS18: High ratio (and high pressure) and low ratio. Cooling down the cryoinserts changes the gas composition from high to low ratio.

Variation of Intensity and Ramping Rate

Before and after each cooldown, i.e. at warm and cold cryoinserts, the intensity dependent transmission for different ramping rates of normal production cycles were measured. Due to increasing charge exchange rates and self amplification, the dependence of extracted particles on the number of

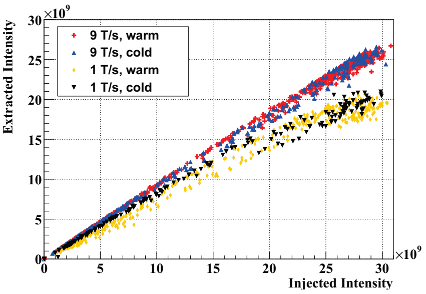

Figure 7: Extracted beam intensity as function of injected beam intensity for different ramping rates as well as for warm and cold cryoinserts.

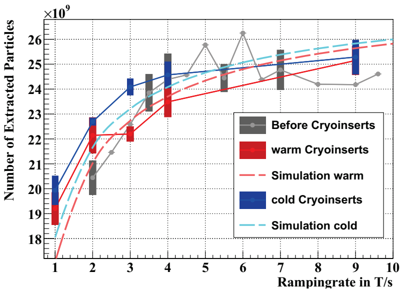

Figure 8: Maximum extracted number of particles as a fuction of the ramping rate for warm and cold cryoinserts. „Before Cryoinserts“ data are from 2023 [2] and restricted to the available intensity in 2025.

injected particles becomes nonlinear above a certain intensity. In Fig. 7 these data are shown. At low ramping rates, a saturation is visible. Cold cryoinserts yield in slightly higher extraction intensities at high injected intensities. As the available intensity during 2025's machine development beam time was limited to $3 \cdot 10^{10}$ injected particles, for high ramping rates no saturation is visible yet. Nevertheless, the data with cold cryoinserts exceed data with warm cryoinserts.

In Fig. 8 the dependence on the ramping rate was analyzed using only the cycles with highest intensity . Cooling down the cryoinserts results overall in a slightly increased intensity. The data shown from 2023 [2] were taken before the cryoinsert's installation and are restricted to the 2025-intensities. Although a higher intensity was available at that time, obviously the machine settings were less optimized.

The different types of losses during a cycle were analyzed for Fig. 9, as already presented in [2]. Here, cycles with warm and cold cryoinserts are compared. Injection loss, Rf-capture-loss and losses during injection plateau are unaffected by the cryoinsert's temperature. But as expcected, the losses during acceleration ramp decrease with cooled cryoinserts.

SIMULATION

As the StrahlSim code [9] was used to predict improvements by cryogenic surfaces [7], the same code will be used to understand the measurements with the cryoinserts. This requires a detailed understanding of the vacuum system, which serves as a basis for the simulations. Aging effects of NEG-surfaces as well as increased outgassing areas due to different installations or leaks have to be considered to reproduce a measured pressure profile consisting of 29 points along the ring. Pressure gauges show a Nitrogen-equivalent, therefore the total pressure from a simulation has to be converted accordingly for being compared to a measurement. As learned from Fig. 6, the rest gas composition is not constant along the ring, but also comes as an adjustable parameter into the simulation. Also the charge exchange cross section [8] are based on a theoretical model subjected to uncertainties.

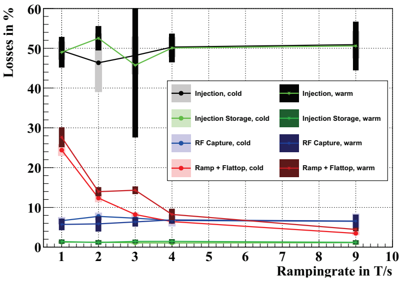

Figure 9: Analysis of different beam loss mechanisms during acceleration cycles for warm and cold cryoinserts. Charge exchange losses happen during ramping. Here the cold cryoinserts decrease the amount of beam loss.

Using an adopted vacuum system and an educated guess for the residual gas composition, energy dependent lifetime measurements in a static vacuum can be reproduced. Increasing the intensity and going to dynamic vacuum requires all available parameter within the simulation, which also includes the "history" of a vacuum system, i.e. the number of cycles in continuous operation. Results of such simulations are shown in Fig. 8. The agreement with the measurement is available but also shows room for improvement. As explained, many parameters influencing each other influence these results.

SUMMARY AND OUTLOOK

The effect of the cryoinserts on high intensity heavy ion beams could be investigated for the first time. A clear decrease of charge exchange rates by cooling down the cryoinserts could be observed, proving the cryoinserts functionality. It could be shown, that the decrease of pressure also yields in reduced charge exchange beam loss.

In the next steps, the cryoinserts design gets optimized for a series production. The copper sheets not necessarily have to be round, which is difficult to manufacture. Therefore, they will have ten edges in future. Also the areas of thermal contact between components were revised in order to achiever higher surface pressure and such a lower thermal resistances.

REFERENCES

[1] P. J. Spiller, L. H. J. Bozyk, and P. Puppel, “SIS18 – Intensity Record with Intermediate Charge State Heavy Ions”, in *Proc. IPAC’11*, San Sebastian, Spain, Sep. 2011, paper WEPS003, pp. 2484–2486.

[2] L. Bozyk and P. Spiller, “SIS18 Operation with U^{28+}”, in *Proc. IPAC’24*, Nashville, TN, USA, May 2024, pp. 1661–1664. doi:10.18429/JACoW-IPAC2024-TUPS13

[3] L. H. J. Bozyk and P. J. Spiller, “Ionization Loss and Dynamic Vacuum in Heavy Ion Synchrotrons”, in *Proc. IPAC’17*, Copenhagen, Denmark, May 2017, pp. 2201–2204. doi:10.18429/JACoW-IPAC2017-TUPVA056

[4] L. H. J. Bozyk, S. Aumüller, and P. J. Spiller, “Cryogenic Surfaces in a Room Temperature SIS18 Ioncatcher”, in *Proc. HIAT’22*, Darmstadt, Germany, Jun.-Jul. 2022, pp. 79–82. doi:10.18429/JACoW-HIAT2022-TUP06

[5] L. Bozyk, S. Aumüller, and P. Spiller, “Cryogenic surfaces in a room temperature SIS18 ion catcher”, in *Proc. IPAC’23*, Venice, Italy, May 2023, pp. 4283–4286. doi:10.18429/JACoW-IPAC2023-THPA139

[6] L. Bozyk and P. Spiller, “Cryogenic inserts in the room temperature synchrotron SIS18 at GSI”, in *Proc. IPAC’25*, Taipei, Taiwan, Jun. 2025, pp. 3094–3097. doi:10.18429/JACoW-IPAC2025-THPS058

[7] L. H. J. Bozyk and P. J. Spiller, “Measurement of Beam Ioniziation Loss in SIS18”, in *Proc. IPAC’14*, Dresden, Germany, Jun. 2014, pp. 864–866. doi:10.18429/JACoW-IPAC2014-MOPRI104

[8] L. Bozyk, F. Chill, M.S. Litsarev, I.Yu. Tolstikhina and V.P. Shevelko, “Multiple-electron losses in uranium ion beams in heavy ion synchrotrons”, *Nucl. Instrum. Methods Phys. Res.*, Sect. B, vol. 372, pp. 102-108, 2016. doi:10.1016/j.nimb.2016.01.047

[9] P. Puppel, “Orts- und zeitaufgelöste Simulation strahlinduzierter dynamischer Vakuumeffekte in Schwerionensynchrotrons”, Ph.D. thesis, Physics Department, Goethe Universität Frankfurt, Frankfurt, Germany, 2012